Electronic Supplementary Material (ESI) for RSC Advances.

A F-ion Assisted Preparation Route to Improve the Photodegradation Performance of TiO_2@rGO System-How to Efficiently Utilize the Photogenerated Electrons in the Target Organic Pollutants

Linjuan Guo,[a,b] Zheng Yang,[a, b] Baiyi Zu,[a] Bin Lu,[a] and Xincun Dou[a]*

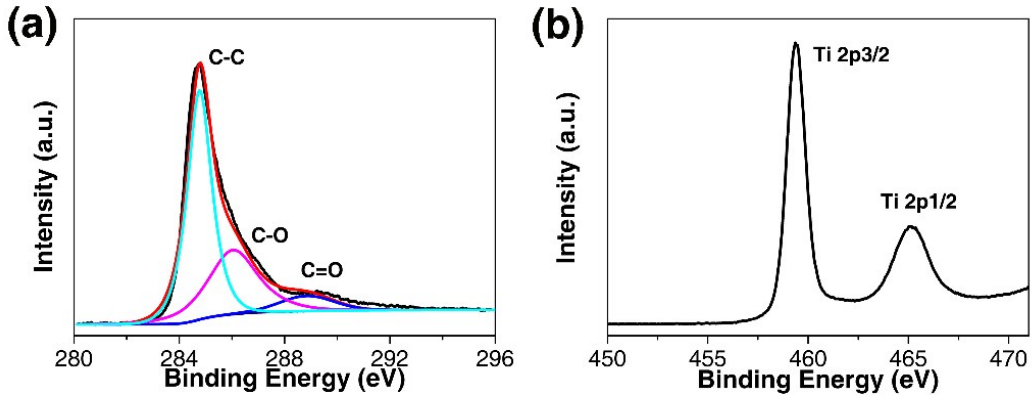

Figure S1. (a) C 1s and (b) Ti 2p XPS spectra of the F-doped TiO_2@rGO heterojunction.

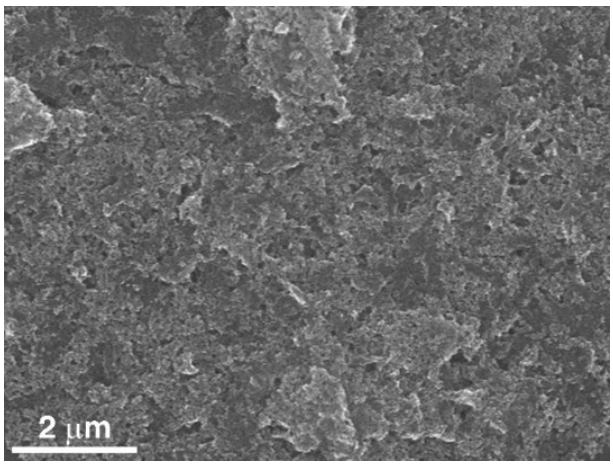

Figure S2. SEM image of the F-doped TiO_2@rGO heterojunction.

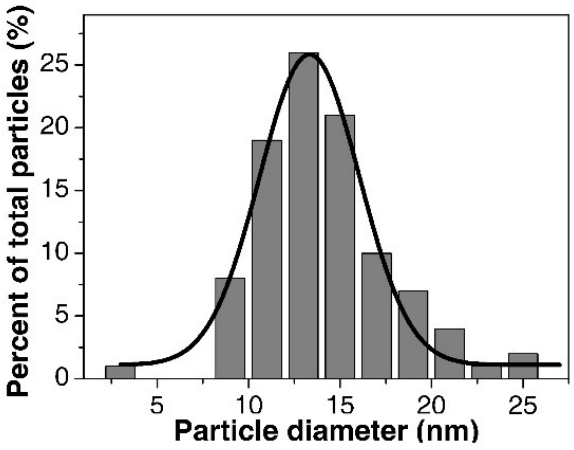

Figure S3. The size distribution of the TiO_2 nanocrystals of the F-doped TiO_2@rGO heterojunction.

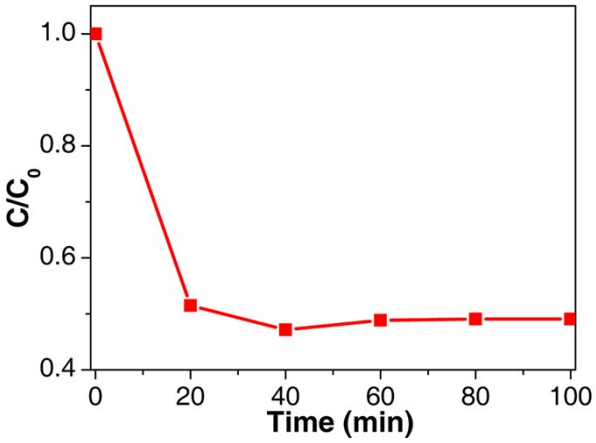

Figure S4. The adsorption equilibrium curve of RhB solution with time in dark.

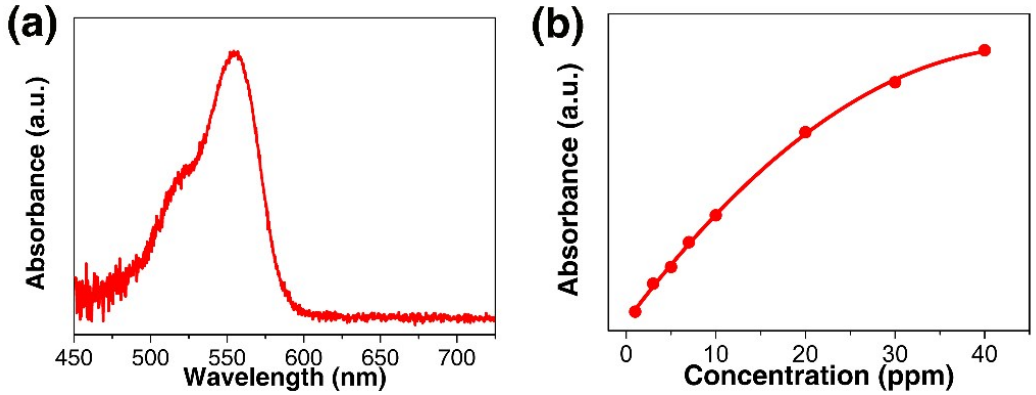

Figure S5. a) UV-vis absorption spectrum of RhB; b) Fitting curve of UV-vis absorption spectrum of different concentrations of RhB (2-40 mg/L).

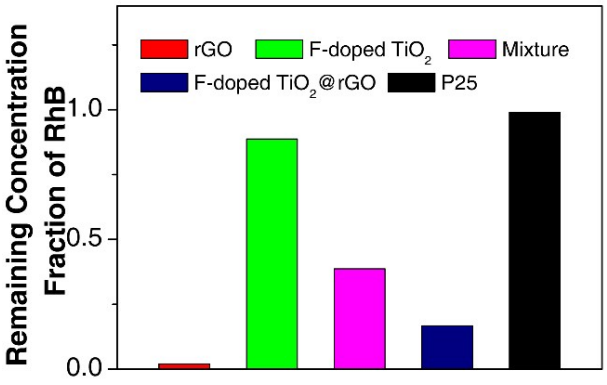

Figure S6. Bar plot showing of the remaining RhB in solution after reaching the adsorption equilibrium in dark of rGO, F-doped TiO_2, the mixture, F-doped TiO_2@rGO and P25.

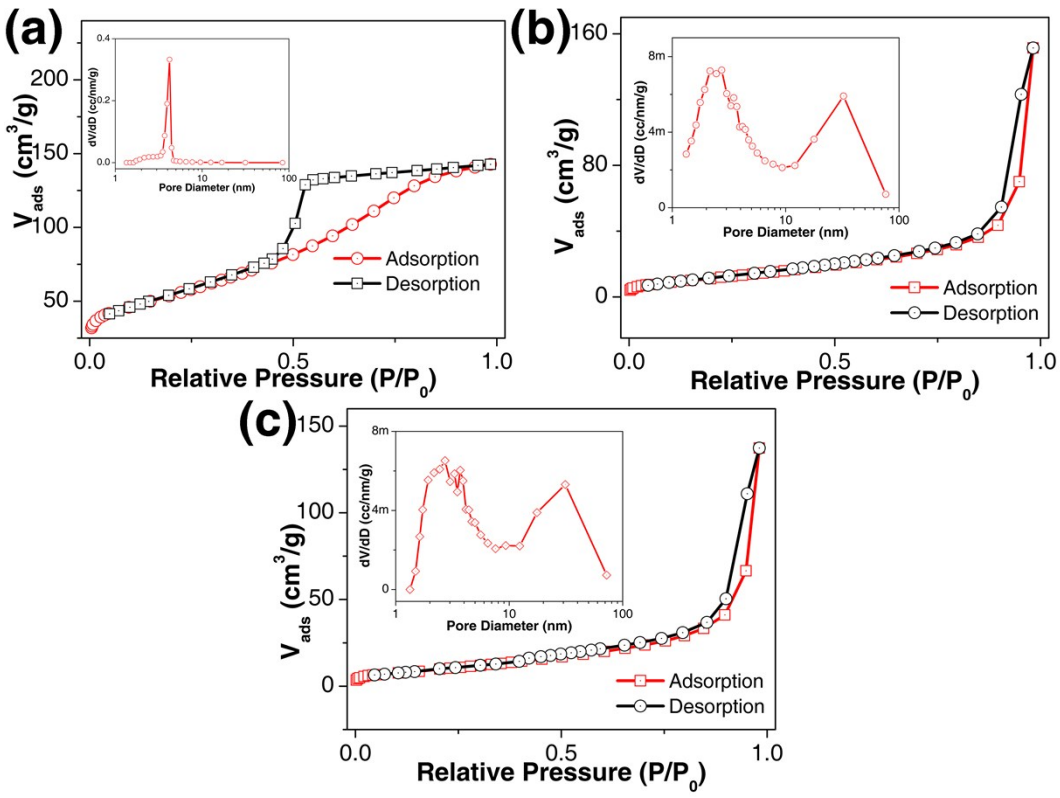

Figure S7. N_2 adsorption-desorption isotherms of (a) the F-doped TiO_2@rGO heterojunction, (b) F-TiO_2 and (c) the mixture, insets are the corresponding pore size distributions. They all resemble the Type IV.[1]

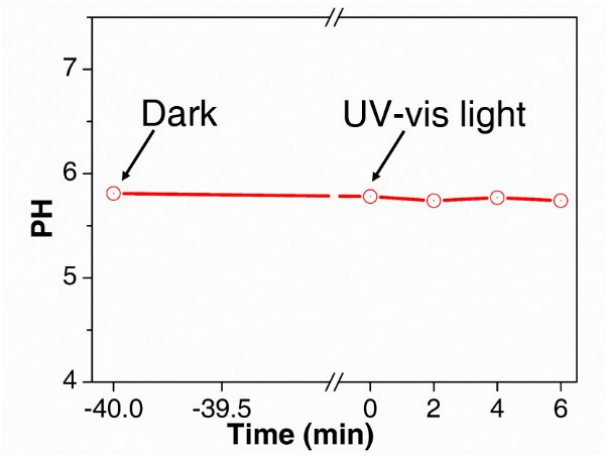

Figure S8. The pH value in the liquid-phase of F-doped TiO_2@rGO heterojunction towards RhB with time under dark and UV-vis light irradiation.

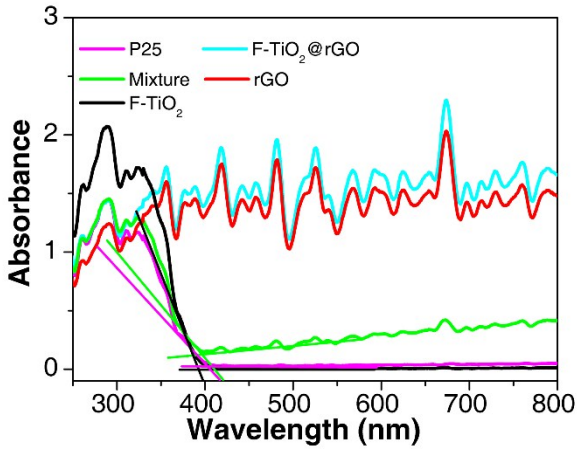

Figure S9. UV-vis diffuse reflectance spectra of rGO, F-doped TiO_2, the mixture, F-doped TiO_2@rGO and P25.

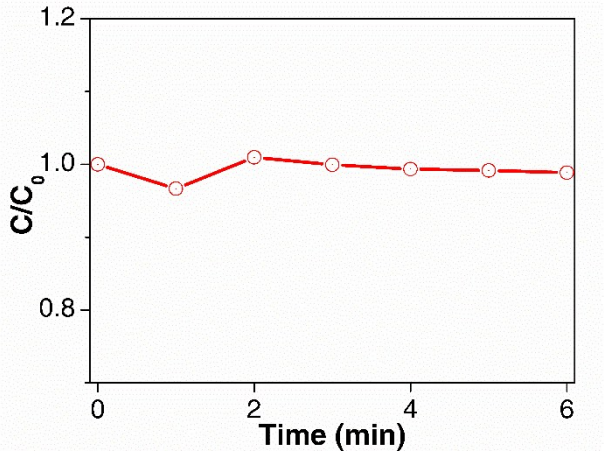

Figure S10. The stability of RhB with time under UV-vis light irradiation ($300 \leq \lambda \leq 2500$ nm).

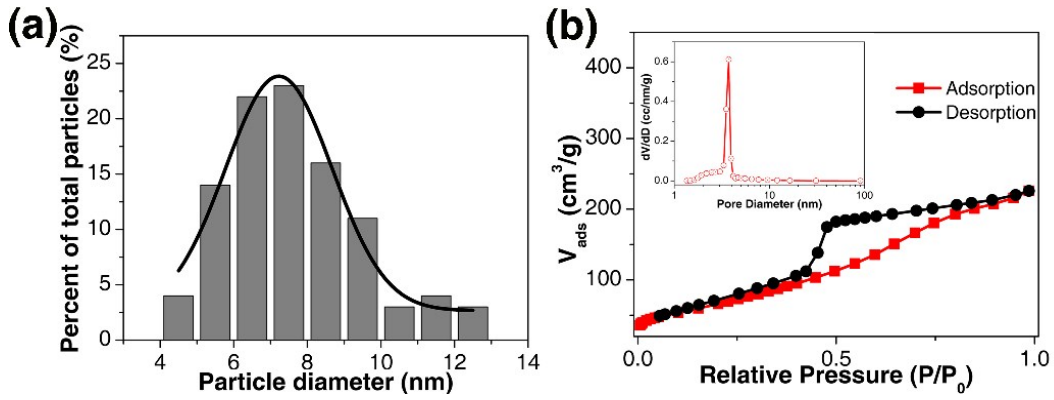

Figure S11. (a) The size distribution of the TiO_2 nanocrystals and (b) N_2 adsorption-desorption isotherm of the pure TiO_2@rGO heterojunction, inset is the corresponding pore size distribution.

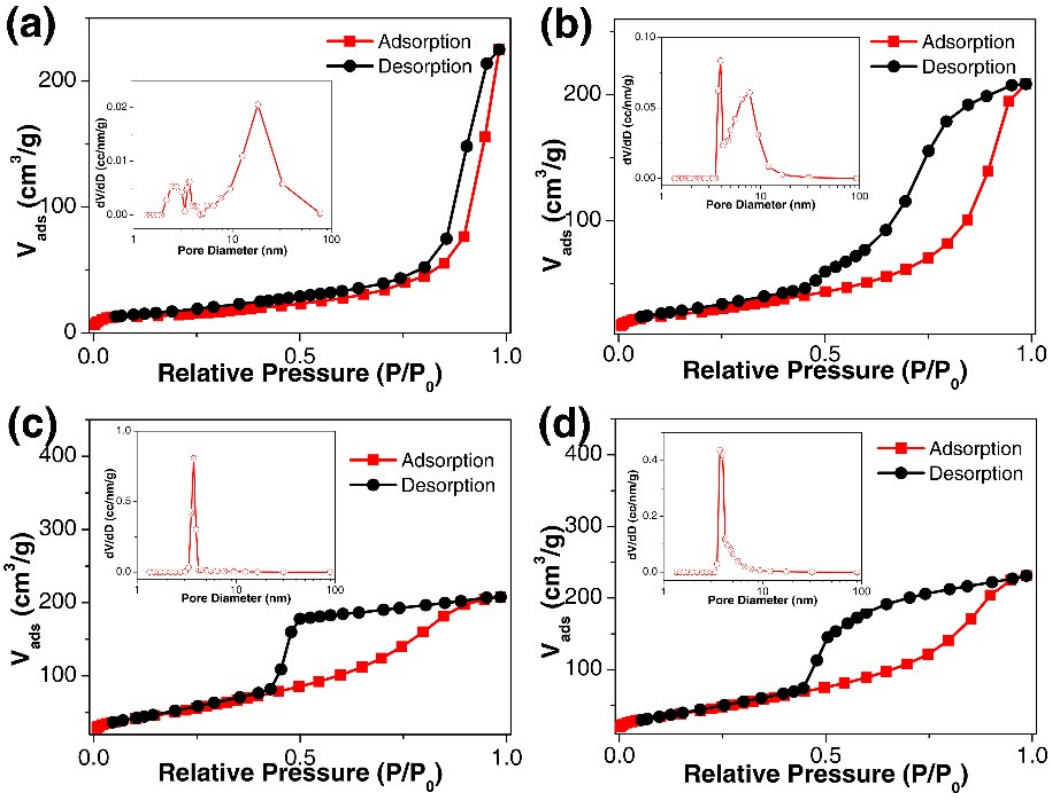

Figure S12. N_2 adsorption-desorption isotherms of the F-doped TiO_2@rGO heterojunction with different weight ratios of rGO ((a) 1%, (b) 5%, (c) 13% and (d) 15%), insets are the corresponding pore size distributions.

Table S1. Average grain size of the TiO_2 nanocrystals in the F-doped TiO_2@rGO heterojunction calculated by Scherrer formula in different diffraction planes.

Diffraction plane	F-doped TiO_2@rGO (nm)
(101)	12.11
(004)	14.97
(105)	26.49
(211)	22.83

Table S2. Surface area and average pore diameter of the F-doped TiO_2@rGO heterojunction, F-TiO_2, and the mixture (F-TiO_2@rGO).

	Surface area (m^2/g)	Average pore diameter (nm)
F-doped TiO_2@rGO	192.6	4.58
F-TiO_2	44.6	2.1
Mixture	39.4	2.16
Pure TiO_2@rGO	262.6	5.32
F-doped TiO_2@(rGO-1%)	53.2	26.2
F-doped TiO_2@(rGO-5%)	100.6	12.8
F-doped TiO_2@(rGO-13%)	203.4	6.31
F-doped TiO_2@(rGO-15%)	181.7	7.86

1. K. S. W. Sing, D. H. Everett, R. A. W. Haul, L. Moscou, R. A. Pierotti, et al., *Pure Appl. Chem.*, 1985, **57**, 603-619.